

AD_____

Award Number: W81XWH-FEFA-1-F

TITLE: P^c^l[ãäæ^} öQ æ ã * ÁE^} • Á/æ^* ç * ÁU[• æ^Áöæ &^Á'æ} ã *

PRINCIPAL INVESTIGATOR: 0æ[} Å^Ó^æ

CONTRACTING ORGANIZATION: WASHINGTON STATE UNIVERSITY
 PULLMAN WA 99164-0001

REPORT DATE: June 20FF

TYPE OF REPORT: ☐ Preliminary ☒ Final

PREPARED FOR: U.S. Army Medical Research and Materiel Command
Fort Detrick, Maryland 21702-5012

DISTRIBUTION STATEMENT: Approved for public release; distribution unlimited

The views, opinions and/or findings contained in this report are those of the author(s) and should not be construed as an official Department of the Army position, policy or decision unless so designated by other documentation.

REPORT DOCUMENTATION PAGE				Form Approved OMB No. 0704-0188	
Public reporting burden for this collection of information is estimated to average 1 hour per response, including the time for reviewing instructions, searching existing data sources, gathering and maintaining the data needed, and completing and reviewing this collection of information. Send comments regarding this burden estimate or any other aspect of this collection of information, including suggestions for reducing this burden to Department of Defense, Washington Headquarters Services, Directorate for Information Operations and Reports (0704-0188), 1215 Jefferson Davis Highway, Suite 1204, Arlington, VA 22202-4302. Respondents should be aware that notwithstanding any other provision of law, no person shall be subject to any penalty for failing to comply with a collection of information if it does not display a currently valid OMB control number. PLEASE DO NOT RETURN YOUR FORM TO THE ABOVE ADDRESS.					
1. REPORT DATE (DD-MM-YYYY) 01-06-2011		2. REPORT TYPE Annual Summary		3. DATES COVERED (From - To) 31 MAY 2010 - 1JUN 2011	
4. TITLE AND SUBTITLE Heterobivalent Imaging Agents Targeting Prostate Cancer Training				5a. CONTRACT NUMBER	
				5b. GRANT NUMBER W81XWH-10-1-0481	
				5c. PROGRAM ELEMENT NUMBER	
6. AUTHOR(S) Aaron LeBeau E-Mail: Aaron.Lebeau@ucsf.edu				5d. PROJECT NUMBER	
				5e. TASK NUMBER	
				5f. WORK UNIT NUMBER	
7. PERFORMING ORGANIZATION NAME(S) AND ADDRESS(ES) University of California, San Francisco San Francisco, CA 94103				8. PERFORMING ORGANIZATION REPORT NUMBER	
9. SPONSORING / MONITORING AGENCY NAME(S) AND ADDRESS(ES) U.S. Army Medical Research and Materiel Command Fort Detrick, Maryland 21702-5012				10. SPONSOR/MONITOR'S ACRONYM(S)	
				11. SPONSOR/MONITOR'S REPORT NUMBER(S)	
12. DISTRIBUTION / AVAILABILITY STATEMENT Approved for Public Release; Distribution Unlimited					
13. SUPPLEMENTARY NOTES					
14. ABSTRACT To determine the utility of imaging MT-SP1 in cancer, xenografts of different cancer cell lines were evaluated with near-infrared imaging using a fluorescently labeled probe to visualize active MT-SP1. Subsequent in vitro studies demonstrated a correlation between the MT-SP1/HAI-1 mRNA ratio and probe localization to tumor tissue and cell lines. Antibody radiolabeled with single-photon emitting 111In for computed tomography imaging gave a probe for in vivo MT-SP1 detection and quantitation. Pronounced probe localization was observed in cell line derived xenografts and in a patient-derived xenograft (PDX) model. HAI-1 was found to play an important role in modulating MT-SP1 activity in clonal derived cell lines and xenografts, but not in the PDX model. These data show the value of using PDX models to recreate the intrinsic tumor heterogeneity of human cancers and in the development of probes for the non-invasive imaging of cancer.					
15. SUBJECT TERMS No subject terms provided.					
16. SECURITY CLASSIFICATION OF:			17. LIMITATION OF ABSTRACT UU	18. NUMBER OF PAGES 13	19a. NAME OF RESPONSIBLE PERSON USAMRMC
a. REPORT U	b. ABSTRACT U	c. THIS PAGE U			19b. TELEPHONE NUMBER (include area code)

TABLE OF CONTENTS

INTRODUCTION.....	1
BODY.....	3
KEY RESEARCH ACCOMPLISHMENTS.....	6
REPORTABLE OUTCOMES.....	6
CONCLUSION.....	7
REFERENCES.....	7
APPENDICES.....	9

Heterobivalent Imaging Agents Targeting Prostate Cancer

Introduction

Prostate cancer is uniformly lethal once it has escaped the confines of the prostate gland, resulting in the deaths of ~25,000 American men each year. Unlike most solid tumor types, a unique attribute of prostate cancer is the almost universal development of osteoblastic bone metastases in men failing androgen ablation therapy (1, 2). Currently, the ^{99m}Tc bone scan is the primary imaging modality used to evaluate the extent of prostatic disease and the response to therapy. Although the bone scan can measure the number of metastatic sites, it is relatively insensitive, detecting metastases at a relatively late stage. In addition, it is difficult to accurately quantify response to therapy in “real-time” using bone scans (3). Thus far, an accurate and reliable method to image prostate cancer micrometastases and response following therapy does not exist.

One hallmark of cancer cells, when compared to non-malignant cell types, is increased extracellular proteolysis mediated by the over-expression of transmembrane proteases on the cell surface. Two proteases that are over-expressed on the surface of prostate cancer cells are membrane-type serine protease 1 (MT-SP1), also referred to as matriptase, and the aforementioned PSMA. MT-SP1 is a type II transmembrane serine protease that has been implicated as a salient player in the pathobiology of cancers of epithelial origin, e.g. prostate, cervix, ovarian, colon and gastrointestinal (4). Current findings indicate that MTSP1 may play a role in growth factor activation, receptor activation and inactivation, ectodomain shedding and protease activation cascades. MT-SP1 over-expression is strongly prognostic for prostate cancer with high MT-SP1 levels directly correlating to a tumor type with a higher Gleason score (5). PSMA, a type II transmembrane metalloprotease, is expressed in normal prostate epithelial cells

at low levels, but in prostate cancer PSMA levels on the cell surface are increased more than 100-fold (6). The role PSMA plays in cancer progression is unknown and so far no *in vivo* substrates for it have been determined. PSMA is known to function as a carboxypeptidase; acting as a folate hydrolase cleaving poly- γ -glutamated folates and as an N-acetylaspartylglutamate (NAAG) hydrolase (7). Much like with MT-SP1, increased levels of PSMA correlate with a more aggressive cancer phenotype and following androgen ablation therapy, PSMA protein levels either remain the same or increase (6).

In the Craik laboratory, in collaboration with the laboratories of Professor Henry VanBrocklin (UCSF) and Professor Cliff Berkman (Washington State University), we are developing novel imaging platforms for the imaging of MT-SP1 and PSMA *in vivo*. Phage display has allowed the isolation of new antibody-based antagonists that are highly potent for MT-SP1. With K_i values in the picomolar range for MT-PS1, these antibodies show no appreciable inhibition against a panel of closely related serine proteases (factor Xa, thrombin, KLK1, tPa and uPA) (8). The structures of the antibodies can be manipulated to produce the full length IgG at 150 kDa, an Fab at 50 kDa or a 30 kDa scFv. Such antibodies for MT-SP1 have been fluorescently labeled in the Craik lab and have demonstrated utility as probes for MT-SP1 *in vivo* and *in vitro*. It is believed that our antibodies can be radiolabeled and find utility as PET and SPECT imaging agents. Additionally, the phosphoramidite compounds developed by Berkman, et.al, have been successfully employed to image PSMA with PET (9). The goal of this fellowship is to create a heterobivalent imaging agent for prostate cancer that targets PSMA and MT-SP1 in the same molecule. To accomplish this, molecules will be made that contain MT-SP1 antibodies tethered to small-molecules PSMA inhibitors that contain imaging moieties.

Our aims were:

1. Find cells lines that express sufficient levels of MT-SP1 on the cell surface that could be imaged using our probe
2. Perform *in vivo* small animal molecular imaging of MT-SP1 with anti-MT-SP1 antibodies in xenografts of human cancer
3. Evaluate *ex vivo* the ability of small-molecule inhibitors to bind PSMA in frozen prostate cancer tissue sections.

Body

Before synthesizing heterobivalent imaging agents for the imaging of prostate cancer, the first experiment required was to see if the MT-SP1 antibodies could be used to image any prostate cancer cell lines *in vitro* and/or *in vivo*. Extensive work has been performed by the Berkman on imaging cells *in vitro* with the PSMA inhibitor, so this work was not replicated by us. The *in vivo* NIR imaging of MT-SP1 in a luminal A breast cancer xenograft using A11 IgG labeled with AlexaFluor 680 (A11-AF680) has been reported previously (10). Building on this, the broad applicability of A11-AF680 at detecting active matriptase *in vivo* in different human cancers and cancer subtypes was determined. NIR optical imaging was used to survey eight different adenocarcinoma xenografts (n = 3 mice/xenograft) (Fig. 1.). The eight different xenografts examined include colon (HT29 and SW620), breast (MDA-MB-231 and MDA-MB-468), prostate (LNCaP, PC3 and DU145) and ovarian cancer (OVCAR-5). The mice were injected with A11-AF680 and imaged out to 120 hours to assess tumor localization and bio-distribution. Full length IgG antibodies have molecular weights around 150 kDa and long *in vivo* half-lives from days to weeks, thus necessitating imaging at later time points. Maximum probe uptake and

retention was observed in the HT29 xenograft at 72 hrs. Probe localization was also observed in the MDA-MB-468 xenograft, but it was minimal when compared to HT29 and only slightly above background. Uptake over background was not observed in any of the other xenografts, including SW620 which is known to be matriptase negative. At 72 hrs, selected HT29 and SW620 mice were euthanized and the tumors were resected and imaged to see if the labeled IgG had penetrated into the tumor. The resected HT29 tumors showed pronounced probe penetration and fluorescence, while the SW620 showed none.

The lack of uptake in xenografts known to express MT-SP1 was investigated. It was determined that while many xenografts do express and even over-express MT-SP1, these same xenografts expressed high levels of MT-SP1's cognate inhibitor hepatocyte growth factor activator inhibitor-1 (HAI-1). MT-SP1 and HAI-1 are co-expressed on the surface of epithelial cells and when high levels are high, little MT-SP1 mediated proteolysis is observed. During the progression of some cancers, such as colon cancer, the ratio of MT-SP1 to HAI-1 is known to increase leading to increased MT-SP1 levels and more MT-SP1 mediated proteolysis on the absence of HAI-1. The mRNA levels of MT-SP1 and HAI-1 were analyzed to determine if the ratio of MT-SP1 to HAI-1 mRNA correlated with probe localization in the previous NIR experiment. A qPCR analysis documented that HT29 had the highest level of MT-SP1 mRNA present (Fig. 2). The triple-negative breast cancer (TNBC) cell line MDA-MB-468 expressed the third highest amount of MT-SP1 mRNA, nearly equal to HT29. The prostate cancer xenograft LNCaP expressed five times less MT-SP1 than HT29, while both PC3 and DU145 produced minute quantities of MT-SP1. The other TNBC cell line MDA-MB-231 and the ovarian cancer cell line OVCAR-5 were found not to express MT-SP1 or HAI-1 mRNA. The three cell lines that expressed the most MT-SP1 also expressed the highest levels of HAI-1 mRNA with MDA-

MB-468 nearly producing twice as much as HT29 and HT29 OxR. HT29 had a MT-SP1/HAI-1 mRNA ratio > 1 with its ratio around 2. Because of its high levels of HAI-1, the ratio for MDA-MB-468 was only 1.1. Three of the cell lines LNCaP, PC3 and DU145, were found to make more HAI-1 mRNA than MT-SP1 mRNA resulting in a matriptase/HAI-1 mRNA ratio < 1 . A ratio of > 1 was found to correlate with probe uptake in the NIR experiment. From these data, it was concluded that no probe uptake was observed in the prostate cancer xenografts because all of the MT-SP1 found in the xenografts was probably inactive due to the fact that it was complexed with HAI-1. Since this antibody probe is specific only for active MT-SP1 that was uninhibited by HAI-1, it can be surmised that no active MT-SP1 was present in the LNCaP, DU145 and PC3 xenografts.

Active MT-SP1 was found in the colon cancer HT29 xenograft. This xenograft was tested, along with a patient-derived xenograft (PDX) model, with SPECT imaging. The $^{111}\text{InCl}_3$ labeling yield of A11-DOTA to create $^{111}\text{In-A11}$ was found to be 87% with a radiochemical purity of the final injected product greater than 97%. Mice were imaged with a small animal SPECT/CT starting 24 hours post-injection (Fig. 3.). In the HT29 xenograft, maximum tumor uptake was observed at 72 hrs with noticeable secondary accumulation in the liver. Ecotin, a macromolecular protease inhibitor originally isolated from bacteria in the human gut, inhibits several serine proteases. Ecotin-RR, engineered as a selective competitive inhibitor of matriptase with a K_i value in the low picomolar range, was administered to the HT29 xenograft mice to block the uptake of $^{111}\text{In-A11}$. Ecotin-RR effectively blocked uptake of the probe in the HT29 xenograft. No probe uptake was observed in the control SW620 mice at 72 hrs. The PDX model was created using resected tumor tissue from the hepatic metastases of colon cancer patients. The tumor tissue was implanted, grown and serially passaged in mice. The ability of PDX models to

reproduce the diversity observed in human tumors has been validated. At 72 hrs, ^{111}In -A11 showed pronounced uptake in the PDX tumor with little secondary uptake in other organs. Following probe wash out, the PDX mice were euthanized and their tumors were harvested. Immunofluorescence using A11-AF488 was performed on tumor sections to detect active matriptase. Active matriptase was detected in all of the sections from the mice ($n = 3$).

For PSMA, one of the compounds synthesized by the Berkman group was labeled with the fluorophore Cy5.5. This compound was incubated with a tissue section from a grade 3 prostate cancer section (Fig. 4). The fluorophore labeled compound was incubated with the tissue for 1hr at RT in a buffer of 5% BSA in PSA. Following that, the slide was washed with PBS 3x and the slide was mounted with Prolong-Gold containing DAPI. The section was then visualized on an epifluorescence microscope in the DAPI and Cy5.5 channel. Seen is an image at 20x magnification.

Key Research Accomplishments

1. mRNA analysis found several cell lines that expressed MT-SP1
2. Molecular imaging (optical and SPECT/CT) was performed on cancer xenografts.
Several xenografts showed uptake and localization, but none were of prostate origin.
3. The small molecule PSMA inhibitor was able to image PSMA in frozen prostate cancer tissue.

Reportable Outcomes

Research that has been sponsored by this award will be reported in the following: None

Conclusion

While active MT-SP1 was not observed in prostate cancer xenografts, there is a possibility that active MT-SP1 could be seen in other prostate cancer xenografts, if a more thorough examination is undertaken. From our experiences with colon cancer, it was learned that not all clonal derived cell lines express active MT-SP1. Colon cancer patient samples contain a lot of active MT-SP1 and this brings up the debate between clonal derived cell lines and PDX models. It is highly possible that prostate cancer in patients might express high levels of uninhibited MT-SP1, but the clonal derived xenografts do not. That is why we are working at UCSF to create a databank of PDX models for human prostate cancer. By screening prostate cancer tissue microarrays in the future, we should be able to determine whether or not clonal derived cell lines are accurate portrayals of prostate cancer in humans.

References

1. Welsh JB, Sapinoso LM, Su AI, Kern SG, Wang-Rodriguez J, Moskaluk CA, et al. Analysis of gene expression identifies candidate markers and pharmacological targets in prostate cancer. *Cancer Res.* 2001;61(16):5974-8.
2. Ernst T, Hergenhahn M, Kenzelmann M, Cohen CD, Bonrouhi M, Weninger A, et al. Decrease and gain of gene expression are equally discriminatory markers for prostate carcinoma: a gene expression analysis on total and microdissected prostate tissue. *Am J Pathol.* 2002;160(6):2169-80. PMCID: 1850818.
3. Lawrentschuk N, Davis ID, Bolton DM, Scott AM. Diagnostic and therapeutic use of radioisotopes for bony disease in prostate cancer: current practice. *Int J Urol.* 2007;14(2):89-95.

4. Darragh MR, Bhatt AS, Craik CS. MT-SP1 proteolysis and regulation of cell-microenvironment interactions. *Front Biosci.* 2008;13:528-39.
5. Uhland K. Matriptase and its putative role in cancer. *Cell Mol Life Sci.* 2006;63(24):2968-78.
6. Wang X, Yin L, Rao P, Stein R, Harsch KM, Lee Z, et al. Targeted treatment of prostate cancer. *J Cell Biochem.* 2007;102(3):571-9.
7. Silver DA, Pellicer I, Fair WR, Heston WD, Cordon-Cardo C. Prostate-specific membrane antigen expression in normal and malignant human tissues. *Clin Cancer Res.* 1997;3(1):81-5.
8. Farady CJ, Egea PF, Schneider EL, Darragh MR, Craik CS. Structure of an Fab-protease complex reveals a highly specific non-canonical mechanism of inhibition. *J Mol Biol.* 2008;380(2):351-60. PMID: 2478700.
9. Lapi SE, Wahnische H, Pham D, Wu LY, Nedrow-Byers JR, Liu T, et al. Assessment of an 18F-labeled phosphoramidate peptidomimetic as a new prostate-specific membrane antigen-targeted imaging agent for prostate cancer. *J Nucl Med.* 2009;50(12):2042-8.
10. Darragh MR, Schneider EL, Lou J, Phojanakong PJ, Farady CJ, Marks JD, et al. Tumor detection by imaging proteolytic activity. *Cancer Res.* 2010;70(4):1505-12. PMID: 2823079.

Supporting Data

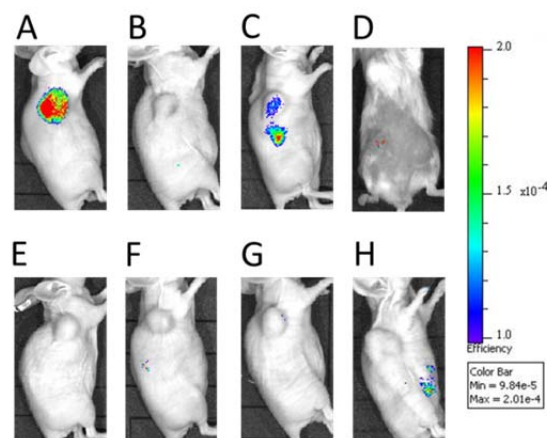


Fig. 1. NIR optical imaging of adenocarcinoma xenografts using A11-AF680. Eight different cancer xenografts, A. HT29 (colon), B. SW620 (colon), C. MDA-MB-468 (breast), D. MDA-MB-231 (breast), E. OVCAR5 (ovarian), F. LNCaP (prostate), G. PC3 (prostate), and H. DU145 (prostate) were imaged with A11-AF680 at 72 hrs post-injection. HT29 was the only xenograft that showed significant tumor uptake and retention at 72 hrs. The other colon cancer xenograft, SW620, is negative for matriptase and did not display probe accumulation.

Fig 2. qPCR of the different cancer lines investigated.

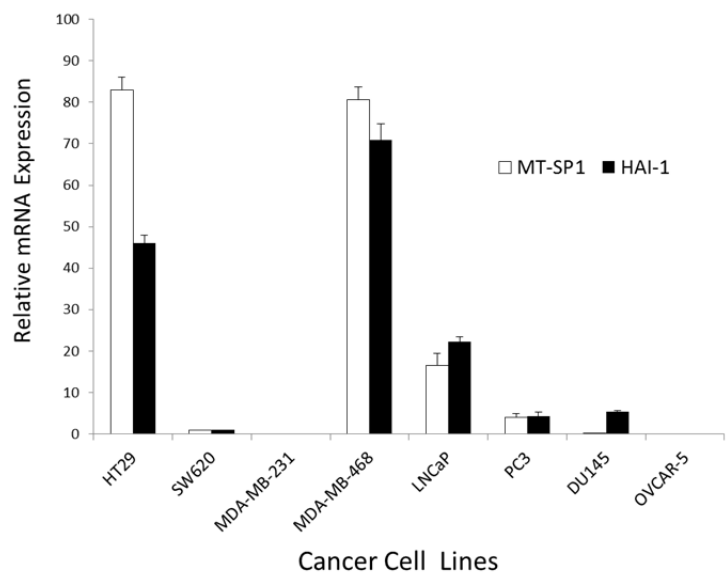


Fig. 3. SPECT nuclear imaging of active matriptase in colon cancer mouse models. ^{111}In -A11 was administered to a (A) HT29 xenograft, (B) HT29 xenograft pre-injected with the macromolecular matriptase inhibitor Ecotin-RR and (C) a PDX model derived from resected human tumor tissue. (A) The probe shows excellent uptake in the HT29 xenograft, with secondary signals coming from the liver and lungs. (B) Uptake of the probe can be blocked in the HT29 xenograft by the pre-injection of ecotin engineered to be selective for matriptase. (C) The probe accumulates preferentially in the PDX tumor. All of the images were acquired 72hrs post-injection and transverse views of the animal. Arrow indicates tumor placement.

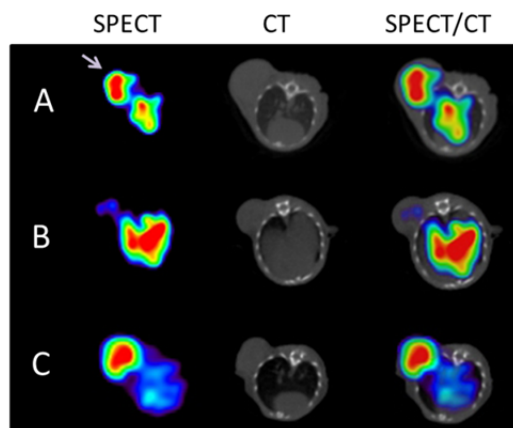


Fig. 4. Imaging PSMA with a small molecule in a Grade 3 prostate cancer section.

